Syracuse University
SURFACE

Biology College of Arts and Sciences

3-1979

Motility of the Microtubular Axostyle in Pyrsonympha

George M. Langford
Syracuse University

Shinya Inoué

Follow this and additional works at: https://surface.syr.edu/bio

 Part of the Biology Commons

Recommended Citation

Langford, G. M., and S. Inoué. 1979. "Motility of the Microtubular Axostyle in Pyrsonympha." The Journal of Cell Biology 80 (3): 521–38.

This Article is brought to you for free and open access by the College of Arts and Sciences at SURFACE. It has been accepted for inclusion in Biology by an authorized administrator of SURFACE. For more information, please contact surface@syr.edu.

MOTILITY OF THE MICROTUBULAR AXOSTYLE IN *PYRSONYMPHA*

GEORGE M. LANGFORD and SHINYA INOUÉ

From the Department of Anatomy, College of Medicine, Howard University, Washington, D. C. 20059, and the Program in Biophysical Cytology, Department of Biology, University of Pennsylvania, Philadelphia, Pennsylvania 19104

ABSTRACT

The rhythmic movement of the microtubular axostyle in the termite flagellate, *Pyrsonympha vertens*, was analyzed with polarization and electron microscopy. The protozoan axostyle is birefringent as a result of the semi-crystalline alignment of ~2,000 microtubules. The birefringence of the organelle permits analysis of the beat pattern in vivo. Modifications of the beat pattern were achieved with visible and UV microbeam irradiation.

The beating axostyle is helically twisted and has two principal movements, one resembling ciliary and the other flagellar beating. The anterior portion of the beating axostyle has effective and recovery phases with each beat thereby simulating the flexural motion of a beating cilium. Undulations develop from the flexural flipping motion of the anterior segment and travel along the axostyle like flagellar waves. The shape of the waves differs from that of flagellar waves, however, and are described as sawtooth waves. The propagating sawtooth waves contain a sharp bend, ~3 μm in length, made up of two opposing flexures followed by a straight helical segment ~23 μm long. The average wavelength is ~25 μm, and three to four sawtooth waves travel along the axostyle at one time. The bends are nearly planar and can travel in either direction along the axostyle with equal velocity. At temperatures between 5° and 30°C, one sees a proportionate increase or decrease in wave propagation velocity as the temperature is raised or lowered. Beating stops below 5°C but will resume if the preparation is warmed.

A microbeam of visible light shone on a small segment of the axostyle causes the typical sawtooth waves to transform into short sine-like waves that accumulate in the area irradiated. Waves entering the affected region appear to stimulate waves already accumulated there to move, and waves that emerge take on the normal sawtooth wave pattern. The effective wavelengths of visible light capable of modifying the wave pattern is in the blue region of the spectrum. The axostyle is severed when irradiated with an intense microbeam of UV light. Short segments of axostyle produced by severing it at two places with a UV microbeam can curl upon themselves into shapes resembling lockwashers. We propose that the sawtooth waves in the axostyle of *P. vertens* are generated by interrow cross-bridges which are active in the straight regions.

KEY WORDS motility · axostyle · microtubules · *Pyrsonympha* · sawtooth wave · birefringence

Microtubule-containing motile organelles such as cilia and flagella propagate undulatory bending waves along their length. The mechanism of bend formation is thought to be the result of active sliding between adjacent doublet microtubules (for reviews, see references 15, 32). In order for the sliding movements between tubules to produce regular bending waves, however, it is necessary for the sliding to be properly localized and coordinated. Direct evidence concerning the mechanisms that regulate sliding has been difficult to obtain. In cilia and flagella, it has been postulated that the central tubules together with the central sheath and the radial links that join them to the outer doublets are involved in the coordination process (33, 34). How these components might interact to produce a system for the coordination of bending is not understood.

The microtubule-containing organelle known as the axostyle found in certain zooflagellates (8, 9, 10, 11) also propagates undulatory bending waves (18, 19). This organelle is appealing as a model of microtubule-associated movement because of its structural simplicity and large size. Electron microscopy studies show that the motile axostyle in the wood roach protozoans *Saccinobaculus* (19, 24) and the termite protozoans *Pyrsonympha* (4, 7, 13, 18, 20, 30, 31) contains several thousand singlet microtubules interconnected by cross-bridges. The microtubules are organized into rows, and the microtubules within the rows are connected to each other by regularly occurring linkers or intrarow bridges. In turn, the rows of microtubules are interconnected by less regularly occurring cross-bridges or interrow bridges. The intrarow bridges appear periodic along the tubules with a spacing of 16 nm. The interrow bridges are not strictly periodic and can be oriented at varying angles to the axis of the microtubule (3, 24). The axostyle, therefore, is both organizationally simple and contains a small number of accessory components.

The bending of the axostyle in *Saccinobaculus* appears to be accompanied by sliding of rows of microtubules relative to one another (2, 25). This axostyle contains a protein with enzymatic activity and molecular weight that are similar to those of ciliary and flagellar dynein and a protein with a molecular weight similar to that of flagellar nexin (26). The dyneinlike protein is thought to be located in the interrow bridges (2), and the nexinlike protein in the intrarow bridges. The movement of the axostyle in *Saccinobaculus* is interpreted as the propagation of circular arcs down a helical ribbon (25). The axostyle therefore has been shown to have both structural and functional features in common with cilia and flagella.

The motion and organization of the axostyle in *Pyrsonympha* are different from those of the axostyle in *Saccinobaculus*. In *Pyrsonympha*, the rows of microtubules are shorter and more numerous and the bends on the axostyle are separated by long unbent regions (18, 23, 31). The packing order of the microtubules has been shown to differ in the bent and straight regions of the axostyle (31) but a detailed analysis of this bending motion has not been described. In this paper, we show that the axostyle exhibits both cilia- and flagella-like movements and that the undulatory waves are sawtooth in shape. We also describe perturbations of the axostyle's activity, analyze the effects of temperature on the beat characteristics, and report changes in the wave form after blue and ultraviolet microbeam irradiation.

MATERIALS AND METHODS

The termites used in this study were collected along the Atlantic coast from North Carolina to Cape Cod, but primarily in the vicinity of Philadelphia. They were collected in infected wood and stored in plastic boxes in the laboratory.

To release the anaerobic protozoa from the hindgut, the abdomen of a worker termite was placed in a drop of medium on a glass slide and gently opened with fine dissecting needles. This operation was performed in a CO_2 atmosphere to maintain anaerobiosis. The exposed hindgut was then ruptured, releasing its contents into the drop of medium. The drop of medium was covered by a glass coverslip, each corner of which was supported by a small fragment of coverslip to prevent flattening the cells. The edges of the coverslip were sealed to the slide with valap (vaseline, lanolin, paraffin; 1:1:1). Cells could be maintained for several hours in such a preparation before the axostyle beat was noticeably affected.

Another method of preparation involved squeezing the abdomen of the termite with fine-tip forceps, forcing out some of the hindgut content. The droplet of fluid was mixed into a drop of medium on a glass slide, and the preparation sealed with valap. This type of preparation had the advantage of being free of tissue and debris from the termite abdomen which interfered with observations in polarized light. If preparations were sealed quickly enough, a CO_2 atmosphere was not necessary.

The medium routinely used was a modified Hungate

medium formulated by S. Inoué and T. Punnett, according to the rules of Provasoli (28), and contains the following chemicals: 22.5 mM Na_2HPO_4, 1.0 mM $CaCl_2$, 15 mM NaH_2PO, 0.01 mM $MgSo_4$, 10 mM KCl, 0.01 mM $(NH_4)_2SO_4$, 5 μM $FeSO_4$, 1 μM $CuSO_4$, 25 μM H_3BO_3, 1 μM $ZnSO_4$, 1 μM $MnCl_2$, 1 μM MoO_3. This medium was prepared in Ballantine distilled water (1) and the pH was adjusted to 7.0. Human saliva was sometimes used to sustain the cells. Saliva is slightly hypotonic for these cells, and they tend to gradually swell in it.

Observations were made with either a Zeiss Universal phase contrast microscope or a Leitz Ortholux polarizing microscope equipped with American Optical strain-free rectified objectives and condenser. HN22 polaroid sheets (Polaroid, Inc., Cambridge, Mass.) were used for polarizers and ~λ/20 mica plate (Brace-Kohler design) for the compensator. A high pressure quartz mercury arc lamp (HBO/200, Osram), together with heat-absorbing filters (Edmund's Scientific Co., Barrington, N. J.) and monochromatic green multilayer interference filter transmitting the bulk of the mercury 546 nm line (Baird-Atomic, Inc., Cambridge, Mass.), was used.

For studies involving visible light and long wavelength UV microbeam irradiation, a slit several tenths of a millimeter in width was placed at the field stop. The image of this slit projected onto the specimen by the condenser provided the proper size microbeam of ~10 μm. To irradiate, the green interference filter and polarizer, but not the heat-absorbing filter, were removed, thus illuminating the cell with visible white light. The glass lenses, filters and slide effectively eliminated the UV and infrared regions of the spectrum, permitting only light with wavelengths between 320 and 770 nm to pass. For UV studies, the glass condenser was replaced with a quartz condenser, and a quartz coverslip was used instead of a glass slide. To produce the desired effects, the axostyle was irradiated 10–30 s.

Temperature effects were obtained with a temperature-controlled microscope slide through which water of various temperatures was circulated.

Motion pictures of the movement in polarized light were made with an Arriflex movie camera (Arriflex Corp. of America, Westbury, N. Y.). Obtaining sufficient light through the polarizing microscope for proper exposure was a problem. Nevertheless, a framing rate of up to 20/s was obtainable, using Kodak 16-mm Tri-x reversal film processed in Kodak D-19 developer for the recommended time.

Measurements of wave displacement, basal inclination, and velocity were taken from the cine film with a Vanguard motion analyzer. The beat frequency of the axostyle was quantitated with a photomultiplier on the microscope as follows: A photomultiplier tube was attached to the ocular of the polarizing microscope, and a small segment of the axostyle only was illuminated by closing down the field diaphragm. The output of the photomultiplier was amplified by a simple two-step DC amplifier and recorded on a strip chart recorder capable of responding to ~20 cps with a 10-mm pen travel. As the azimuth angle of the illuminated portion of the axostyle changed relative to the polarizer and compensator angles, corresponding to a beat, the brightness of the axostyle changed, and the subsequent intensity variation was recorded on the graph paper. Thereby, each spike on the chart represented a beat.

Cells for electron microscopy were fixed for 1.25 h in a 2% glutaraldehyde solution made up in 0.05 M cacodylate buffer and 1% $CaCl_2$ at pH 7.4. The cells were washed in the cacodylate buffer with $CaCl_2$ plus 10% sucrose for 30 min and postfixed in 1% OsO_4 made up in the same buffer for 45 min. The cells were then dehydrated through a graded series of acetone solutions and, when in 100% acetone, embedded in Araldite. Thin sections were cut on a Sorvall Porter-Blum ultramicrotome II (DuPont Instruments-Sorvall, DuPont Co., Wilmington, Del.), stained with uranyl acetate and lead citrate, and viewed with a Philips EM 200 electron microscope.

RESULTS

Description of the Axostyle

In *Pyrsonympha* (Fig. 1), the axostyle originates from a rodlike structure at the anterior tip of the organism. This curved rod (19) has been shown to contain a single row of cross-bridged microtubules associated with a cross-hatched set of 5- to 10-nm filaments and a pair of centrioles surrounded by dense amorphous material (4, 7, 20, 30). In the phase contrast microscope, the

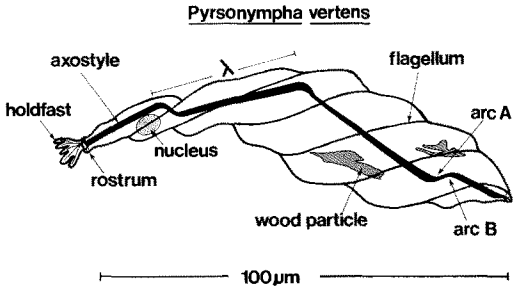

FIGURE 1 A diagram of *P. vertens*. The dominant features of the cell, as seen in the polarizing microscope, are shown. Three waves are depicted on the axostyle. The waves are sawtooth in shape with a sharp bend followed by a long straight region. λ refers to one wavelength. The bends consist of arcs A and B; arc A has a positive radius of curvature, and arc B has negative curvature. The irregularly-shaped objects in the posterior half of the organism are vesicles containing wood particles. Four flagella originate in the rostrum and wrap spirally around the organism. As the organism swims, it rotates about its long axis.

centriolar complex is visible as a 3-μm long, thin rod aligned perpendicular to the long axis of the axostyle (Fig. 2). In the polarizing microscope, this rod is positively birefringent (Figs. 3 and 11). Because it is aligned with its long axis normal (90°) to the length of the axostyle, which is also positively birefringent, the rod appears opposite in contrast to the axostyle. This rodshaped structure is termed the axial ribbon-basal body complex (7) and serves as an important marker for analysis of the axostyle's motion.

The singlet microtubules of the axostyle are aligned parallel to one another along the length of the organelle. In cross-sections of the axostyle, one sees that the microtubules are uniformly distributed in a semicrystalline array (Fig. 4). The microtubules of the axostyle are interconnected by the intrarow and interrow cross-bridges. The axostyle has ~75 rows of microtubules with 25–30 microtubules per row.

In the polarizing microscope, the retardation ([coefficient of birefringence] × [thickness]) of the axostyle is a measure of its thickness in the direction of the light path since the microtubules, which are responsible for the birefringence, have a uniform distribution and, hence, a uniform coefficient of birefringence. Because the axostyle is about three times wider than thick, it appears brighter or darker when it is viewed on its side (its narrow aspect), than when viewed from top or bottom (its wide aspect) (Fig. 3). It is possible to compare maximum and minimum apparent widths with the retardation at the corresponding points on the axostyle. When this is done, one finds that retardation varies inversely with width as predicted.

The axostyle, which measures ~100 μm in length, is helically twisted. The intrinsic twist in the axostyle is shown in the phase contrast micrograph of Fig. 2. One sees, between the two bends in the axostyle of this cell, differences in contrast which correspond to differences in width and thickness of the organelle. These variations in width and thickness result from the fact that the axostyle is helically twisted.

The degree of twist can be ascertained by measuring the distance between a point on the axostyle of maximum and an adjacent one of minimum width, or of minimum and maximum birefringence at a given instant in time. This length constitutes a rotation of 90°. When this measurement is made, the axostyle is found to be intrinsically twisted at a pitch of 133 ± 10 μm, or with an average twist of 2.7°/μm. As a result of the twist on the axostyle, planes defined by, for example, the bend region of two successive waves will be rotated ~68° with respect to one another.

Movements of the Axostyle

Axostyle-associated motility in *P. vertens* is characterized by a rhythmic flipping motion of the anterior region of the organism, and the movement of sharp bends along the helically twisted organelle. From analysis of axostyle movement on cine film (see set of frames in Fig. 3) these activities can be resolved into four basic movements: two primary motions, undulatory and flexual, and two secondary motions, rotational and precessional. The undulatory motion resembles wave propagation along flagella, and the flexual motion simulates the bending of cilia.

THE UNDULATORY AND ROTATIONAL COMPONENTS OF THE MOVEMENT: The undulatory component of the axostyle's motion constitutes the propagation of bending waves at an average frequency of 2/s. The propagated waves most closely resemble sawtooth waves whose wavelength varies between 20 and 35 μm. When actively beating, three or four waves travel along the axostyle at any given time (Fig. 3).

Each sawtooth wave contains a long straight segment which is ~22 μm and a bend which has two circular arcs with a combined arc length of ~3 μm (Fig. 1). The straight region appears to be stiff since it usually shows no tendency to bow. In the bend region, the two arcs are contiguous, one (arc A) having a positive and the other (arc B) a negative radius of curvature (Figs. 1 and 3). Arcs A and B may be functionally identical to the principal and reverse bends of flagellar waves (16). The radius, which averages 1.4 μm, of the two arcs varies independently as the wave propagates. The arcs subtend angles which range between 40° and 60°, and arc A is usually less variable than arc B. This small variation in angle appears to accommodate the cell contour and the ingested wood particles.

As bends propagate, they appear in different orientations as they travel along the twisted axostyle (Fig. 3). The bends are nearly planar and the plane of the bend is perpendicular to the plane which defines the width of the axostyle (Fig. 5) (22). Therefore, when a bend is observed in a region which displays the maximum width of the axostyle, the arcs of the bend are barely detectable (see wave in middle of axostyle in Fig. 3*n–p*).

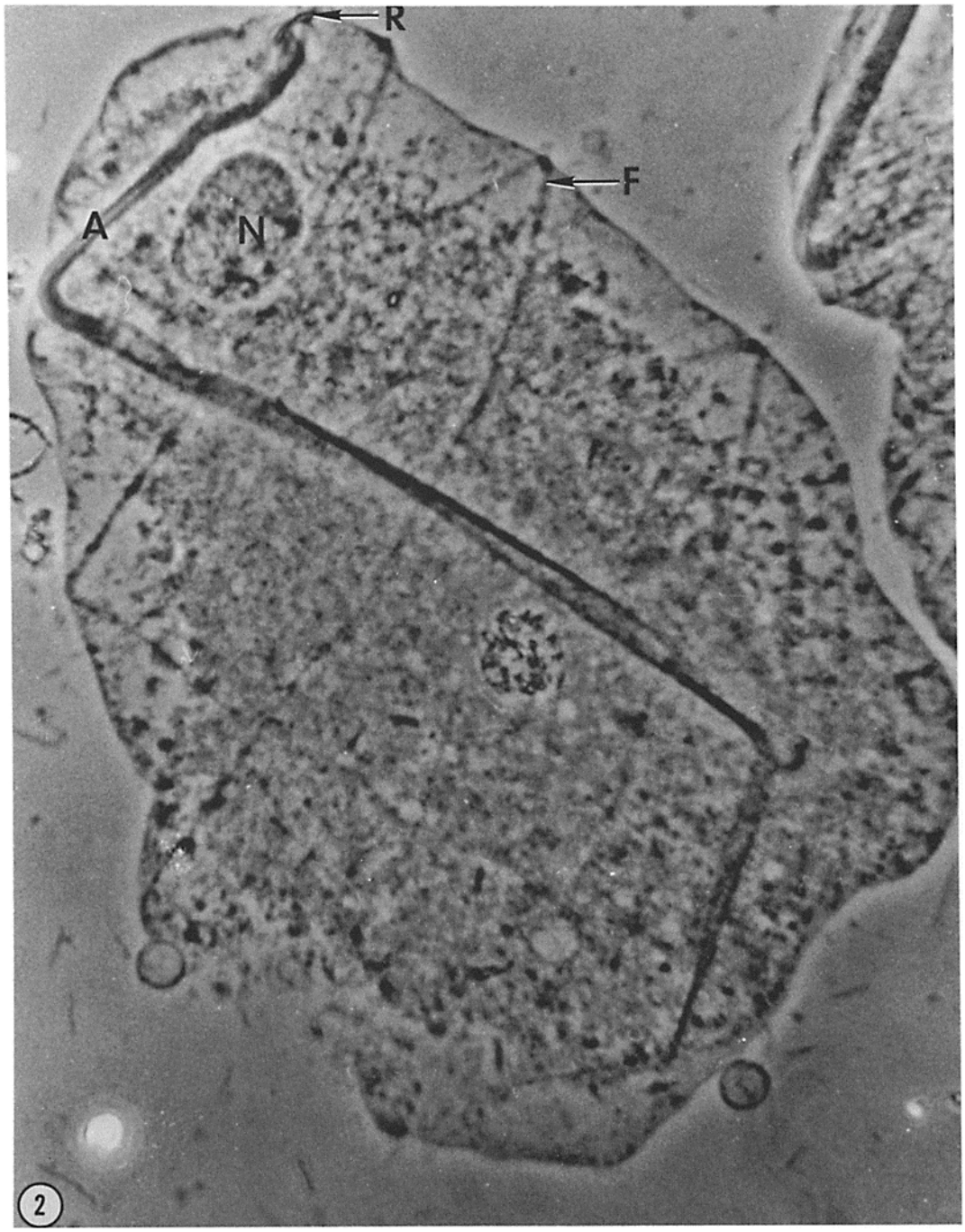

FIGURE 2 Phase contrast micrograph of *P. vertens* showing the helical twist in the axostyle. This cell is flattened to improve the image quality. Flattening prevented the cell from beating, and two inactive bends are present in the axostyle. The twist in the ribbon-shaped axostyle is visible as a variation in width and contrast of the organelle. The axostyle is ~3 × wider than thick. *A*, axostyle; *F*, flagellum; *N*, nucleus; *R*, axial ribbon-basal body complex.

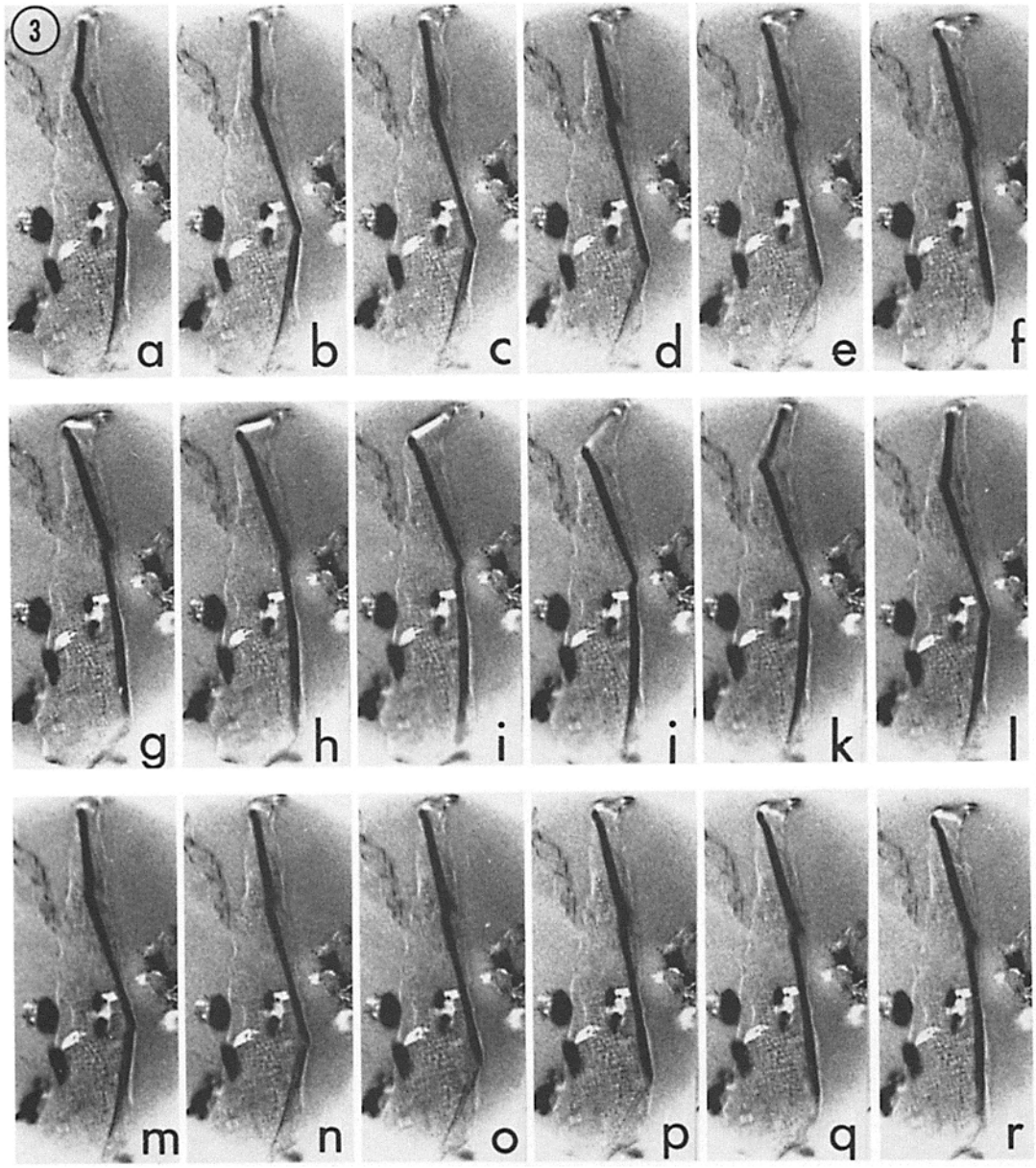

FIGURE 3 Sequential frames from a cine-film made through the polarizing microscope of the beating axostyle in *P. vertens*. The axostyle (see labeled diagram in Fig. 1) is shown in dark contrast. Three waves can be seen on the axostyle. This set of frames follows the movement of these waves through $1^1/_2$ beating cycles. The birefringent particles in the posterior half of the organism are ingested wood particles contained in vesicles. The cell is beating at ~2 beats/s. Filmed at 18 frames/s. × 500.

The small amount of displacement nevertheless seen in the bend region suggests that the bend is not strictly planar and that local bend-associated twisting may take place.

The intrinsic twist in the axostyle appears to dissipate in the region of the bend and reappear after the bend passes (Fig. 3). This untwisting and retwisting is observable as a rolling motion of the

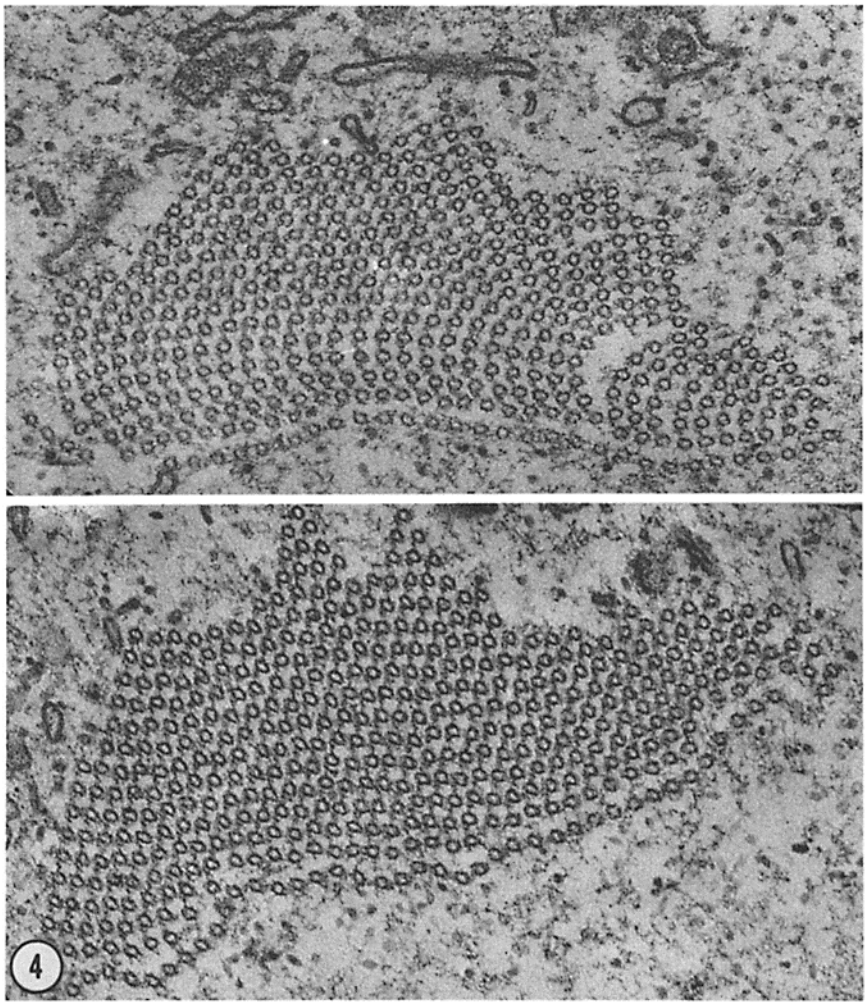

FIGURE 4 Two cross-sections of an axostyle. The microtubules of the axostyle are organized into rows. This axostyle has split into two halves, and only 35 of the 75 rows are shown in these two micrographs. The microtubules within the rows are interconnected by regular intrarow cross-bridges. The rows of microtubules are interconnected by an occasional interrow cross-bridge. The upper micrograph shows the axostyle with curved rows apparently in an unbent region. The lower micrograph, taken farther along the same axostyle and just before a bend was encountered, shows straight microtubular rows. The transition to a straight configuration is presumed to take place in response to bend formation. The number of rows and the number of tubules within a row have changed from the first to the second micrograph. Counting from left to right, row number one is missing in the lower micrograph. Also, row number two of the upper micrograph has one tubule more than the equivalent row of the lower micrograph. The number of tubules in the rows tends to be greater in the upper micrograph, but the number of rows is greater in the lower micrograph with the result that the total number of tubules in each cross-section is almost the same. × 75,000.

axostyle back and forth about its longitudinal axis. This motion is called the rotational component of the axostyle's motion and is classified as a secondary component because it appears to be a consequence of the propagation of the undulatory motion imposed on a helically twisted structure.

The rolling motion is measurable as a change in width of the axostyle as waves propagate. One

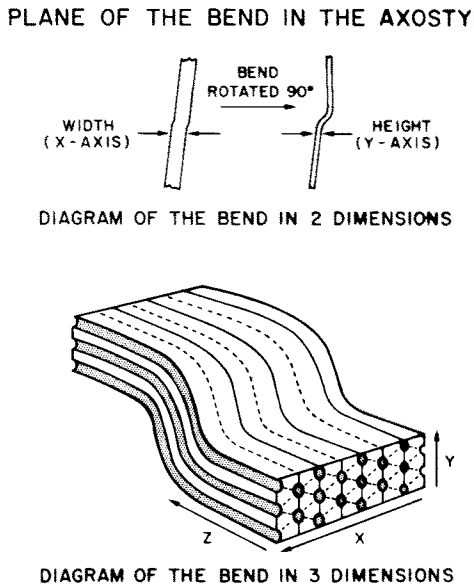

FIGURE 5 Diagram of the plane of the bend in the axostyle of *P. vertens*. In two dimensions, the bend is shown to be almost planar. When the axostyle is viewed with its width to the viewer, the bend is barely visible. When the axostyle is rotated 90°, the two contiguous arcs are seen. In three dimensions, orthogonal axes representing the length, height, and width of the axostyle are shown. A row of microtubules is aligned along the y axis, and the bend is in the y-z plane.

sees a 20% change in width at any given point on the axostyle as a wave approaches and passes that point. The change in width reflects exposure of different aspects of the axostyle which is shaped like a flattened rod with a width-to-height ratio of ~3:1.

In sections through the straight portion of the axostyle, the individual rows of microtubules are all curved, with curvature becoming greater as one progresses from the top of a row (the top of the axostyle is adjacent to the cell surface) to the bottom of it (bound by a row of microtubules set apart from the axostyle proper) (Fig. 10). In sections through the axostyle that are in or near a bend, the rows are not curved but straight (Fig. 4). Apparently, the curvature of the rows, which straightens only in the bend, serves to maintain the stiffness of the axostyle in the unbent regions.

Wave velocity often varies along the length of the axostyle, usually with a maximum velocity approaching 60 μm/s and an average velocity of 40 μm/s at 21° ± 1°C. A typical velocity profile is shown in Fig. 6. The position dependency of velocity is a result of obstructions in the path of the wave. When the wave experiences obstacles such as large cytoplasmic vesicles containing wood chips, neighboring cells, or solid extracellular debris, the velocity decreases. The wave is quite susceptible to impediment for two reasons. Firstly, the wave has a long straight region that is not deformable, and secondly, it follows a helical rather than a straight path. Therefore, when a wave tries to pass an obstruction, it usually cannot do so without a change in wavelength. To achieve this, wave velocity is retarded with a resultant wavelength change. When one wave is impeded, often the effect is transmitted to the oncoming wave. When waves do not experience obstructions, the velocity does not fluctuate along the length of the axostyle but remains constant.

Obstruction to wave passage can be imposed by gently flattening the cell between coverslip and slide. When this is done, an otherwise constant wave velocity can be caused to become variable along the axostyle. A simple reorientation of the cell between coverslip and slide can relieve the obstruction, and the velocity becomes constant again.

THE FLEXURAL AND PRECESSIONAL COMPONENTS OF THE MOVEMENT: The second most obvious movement of the axostyle is the flipping motion of the proximal end. This motion, which occurs with the formation of each new wave, is described as the flexural component of the beating axostyle. This cilialike movement has recovery and effective phases with each beat.

To illustrate this movement, a diagram showing

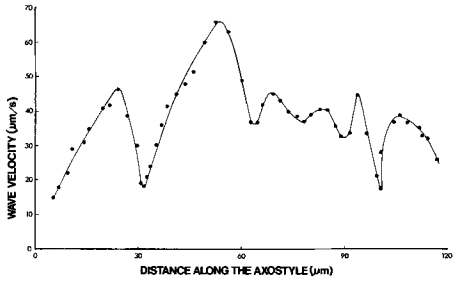

FIGURE 6 Wave velocity profile of bends moving along an axostyle 120 μm long. This record is an average of five successive waves. The velocity varies along the axostyle, producing a pattern that is characteristic for the cell. The variation in velocity is a result of obstructions in the path of the wave (see text). Notice that the velocity is oscillatory along the whole axostyle even though obstructions, as seen from cine-film, only occur at distances of 25 and 95 μm along the axostyle.

a series of profiles of the anterior one-fifth of the axostyle at different time intervals during its beat is given in Fig. 7. Also shown is a graphic record of (*a*) the time change of the angular inclination of the anterior one-fifth of the axostyle with the axial ribbon basal body complex, and (*b*) the position of the bend along the axis of the axostyle. The measurements were made on prints obtained from cine films of the axostyle taken at 18 or 20 frames/s. The detailed timing of the beat of an axostyle is often not constant from on cycle to the next, and so the record given is a typical one, since it is not possible to average out the individual differences between beats.

The recovery phase of the motion involves the initiation and movement of a bend a few micrometers along the axostyle (Fig. 7*a*, times 0 and 0.35 s). During this initial phase of movement the bend contains a single arc only (arc A) which has a

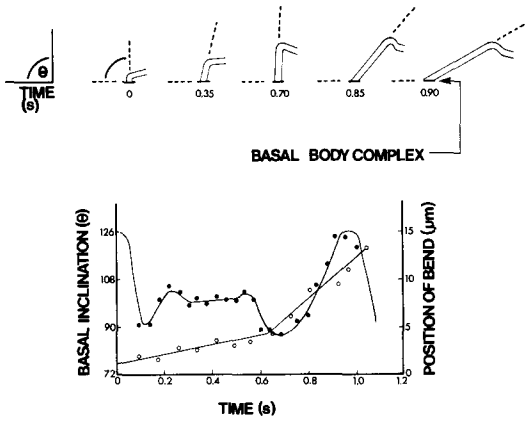

FIGURE 7 A diagram of the cilialike behavior of the anterior segment of the axostyle during the initiation of a wave. (*a*) A diagram of the anterior 1/5 of the axostyle. A thin bar at the base of the axostyle represents the axial ribbon-basal body complex. The angular inclination of the axostyle with the basal body complex is shown at five time intervals. The early phase of the beat (times 0, 0.35, and 0.7 s) is the recovery phase. The effective phase of the beat begins after time 0.7 s. (*b*) A graph of the information depicted in *a* showing the angle Θ, measured in degrees as a function of time (closed circles) and the position of the bend measured in μm, as a function of time (open circles). During the recovery phase, angle Θ increases from 90° to 100° and remains at 100°. Just before the effective phase, angle θ returns to 90° and quickly increases to 126°. Bend displacement (open circles) is diphasic, exhibiting a slow rate during the recovery phase and a fast rate during the effective phase.

"positive" radius of curvature. Just before the onset of the effective stroke, another arc (arc B) with a "negative" radius of curvature appears immediately distal to the initial arc which has now travelled a few micrometers from the proximal tip (Fig. 7*a*, time 0.85 s). With the formation of arc B, the axostyle swings through the effective stroke (Fig. 7*a*, times 0.85 and 0.90 s). The end of the effective stroke occurs with the formation of another bend at the base signalling the formation of a new wave.

The angular inclination of the axostyle to the axial ribbon basal body complex is shown in the graph in Fig. 7*b*. The axial ribbon basal body complex is shown in Fig. 7*a* as a thin rod at the very base of the axostyle aligned perpendicular to its long axis. As is seen in the graph, when the bend is first initiated at time 0.1 s the basal inclination is 90°. It quickly rises to 100° and stays at about this inclination for 0.5 s. Then the inclination quickly falls back to 90° which signals the onset of the effective stroke. This is also the time at which arc B is being formed. After returning to 90° the axostyle swings through the effective stroke forming an angle of 126°. This causes the initiation of another bend. The angle of inclination returns to 90° and the sequence is repeated with each new wave.

The movement of the bend along the axostyle during this flexual motion is not constant, but appears to be diphasic. During the recovery phase of the stroke and when the bend contains only one arc, the bend moves slowly (Fig. 7*b*). However, after the second arc is formed and during the effective phase, the bend moves more rapidly.

The fact that, during the recovery phase, the angle of inclination rises and then falls may be apparent rather than real. It may result from the rotation of the axostyle which affects the measured angle.

The fourth component of the axostyle movement is the precessional component which is exhibited ony at the rostrum. The whole anterior tip of the axostyle, together with the axial ribbon-basal body complex, precesses synchronously with the initiation of each wave. The precessing rostrum sweeps out an ellipse that could well be the compression of a circular path that appears elliptical, because of the orientation of the cell.

These four movements describe the vigorous beating of the axostyle. The flexural motion has the most profound effect on the locomotion of the organism. The cell uses this motion to reorient its

path, particularly when it encounters other cells and debris.

PERTURBATIONS IN THE MOTION OF THE AXOSTYLE: Quite often when preparations are made of *P. vertens,* one observes deviations from the normal behavior associated with the axostyle. Some of these perturbations are described below.

Rotating Polygon Appearance

Sometimes, upon being released from the termite gut, these cells swell and lose their pear shape, becoming partially spherical. This happens frequently when saliva is used as the medium. When the cell takes on a more or less spherical shape, the axostyle is caused to form what approaches a loop. Waves continue to propagate on the axostyle, however. Waves on the axostyle in this configuration give it the appearance of an open rotating polygon (Fig. 8). The wave shape and properties are not affected. The angles of the arcs in the bend region change to accommodate this orientation. Again, arc A is less affected than arc B. At times, arc B is only slightly evident, to the point of being almost absent.

Local Loss of Stiffness

A frequent anomaly that affects the axostyle is the loss of stiffness over a short region. The region affected is usually the same in all cells, and it is the region in the area of the nucleus. The effect of the stiffness loss is to increase the radius of curvature of the bend region of the wave as it passes the affected region and to allow the straight region of the wave to bow (Fig. 8). After a wave passes the affected region, the wave shape returns to normal. The cause of this stiffness loss is not understood.

Reversal of Propagation Direction

Cells that have been beating in culture media for a few hours begin to show a decrease in both beat frequency and propagation velocity. The frequency becomes irregular and waves sometimes stop on the axostyle. On occasion, these waves reverse their propagation direction. Usually, when this occurs, the waves simply back up without any apparent change in the wave shape. In this case, the wave moves towards the basal body with arc A travelling ahead of arc B. On other occasions, the wave shape is seen to reverse before reversal of propagation direction. Velocity in the reverse direction can be as great as in the forward direction. The propagation direction can change back and forth many times, usually with cessation of activity between shifts.

Wave Initiation other than at the Base

Waves can be initiated at any point along the axostyle including the distal end, in which case the waves travel toward the base. Wave initiation other than at the base usually occurs after cells have been in culture medium for a few hours. Most frequently, waves initiate from preexisting waves that are temporarily stopped on the axo-

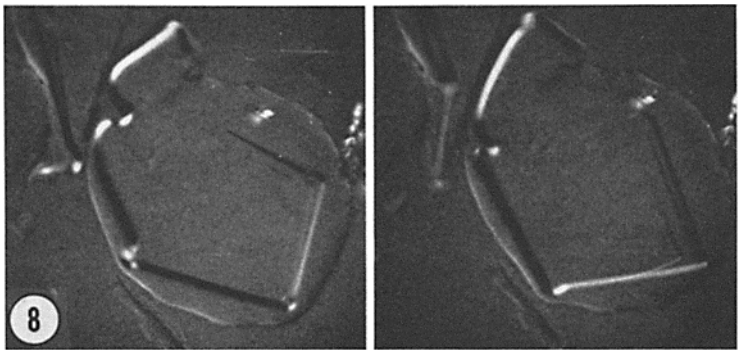

FIGURE 8 Polarized light micrographs of an axostyle. The axostyle has assumed a rotating polygon configuration. Waves continue to propagate along the axostyle in this configuration. They are reminiscent of the movement of the polygons observed by Kamiya (21) in the cytoplasm expressed from the fresh water alga *Nitella.* Note also that the segment between the second and third bends is bowed, appearing to exhibit a local reduction in stiffness. The bends in this region have larger radii of curvature than normal. This stiffness loss is localized to the region including these two bends. Waves past that region have the normal shape. × 500.

style. Many waves can initiate from this site. At other times, waves can be initiated by the axostyle's being deformed, because of contact with neighboring protozoans. In one instance, when a *Trichonympha* bumped into the axostyle of a *P. vertens*, a wave was initiated from that region both towards the centriole and towards the distal end. Sometimes, waves are initiated *de novo*. Wave shape and properties are the same, regardless of the point of origin.

Splitting of the Axostyle into Two or More Parts

Axostyles are frequently seen split into fragments. The splitting occurs along the longitudinal axis. Usually, the first split seen in an axostyle occurs more or less along the center, dividing the axostyle into two halves of equal widths (Fig. 9). These halves often divide several more times. Waves continue to propagate on the fragments. As would be expected, the small fragments are not nearly as stiff as the intact axostyle, and as a result there is a tendency for the straight portion of the wave to bow and for the arcs to take on a larger radius of curvature. Propagation velocity is not affected. Splitting occurs between the microtubular rows (Fig. 10).

Effects of Temperature on the Axostyle Beat

Changes in temperature have an immediate effect on the rate of wave initiation and the propagation velocity. Using a temperature control slide and a photomultiplier to record beat frequency (as described in Materials and Methods), one finds that at temperatures below ~5°C the movement stops altogether, but as soon as the temperature is raised the axostyle starts to beat again, first sluggishly, and then vigorously in the course of a minute or so. Birefringence, however, is not altered by low temperature. In general, at temperatures between 5° and 30°C, one sees a proportionate increase or decrease in wave propagation velocity as temperature is raised or lowered.

After lowering the temperature and then returning it to ambient, propagation velocity usually returns to normal before frequency does. As a result, axostyles recovering from lowered temperature will have only one or two waves travelling on them during the early part of the recovery stage. As the axostyle accommodates to ambient temperature, the number of waves approaches normal. The general wave shape is not affected during this process.

Microbeam Experiments

IRRADIATION WITH VISIBLE LIGHT: Axostyles illuminated with intense visible white light become sluggish and quickly stop beating. By irradiating only a small part of the axostyle with a microbeam of visible light (described in Materials and Methods), a local effect can be produced. When a 10-μm segment of the axostyle is irradiated, the following effect is observed. The waves on the axostyle up to the spot of illumination are not altered. Their shape, wavelength, and propagation are unchanged. At the point of irradiation, however, the shape of the wave changes from a sawtooth to a short wavelength "sinelike" wave,

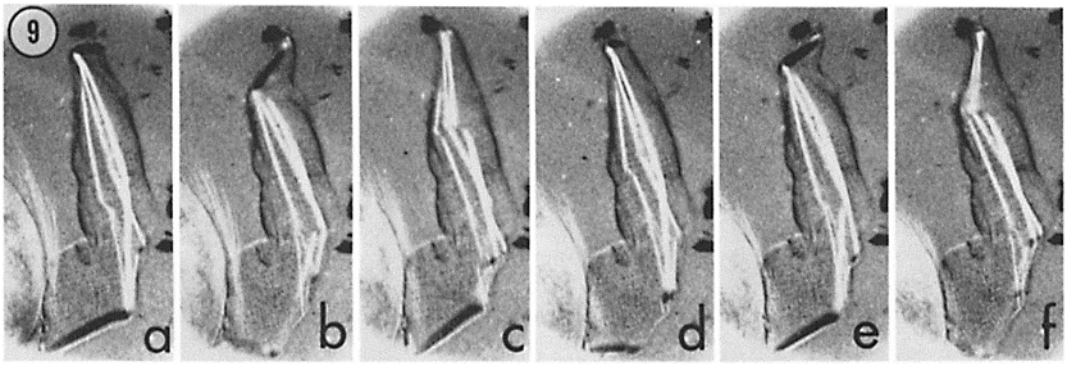

FIGURE 9 Polarized light micrographs of a cell whose axostyle is split along its center into three fragments. The fragments can be seen to beat somewhat out of phase. Sequential frames, 18 frames/s. × 500.

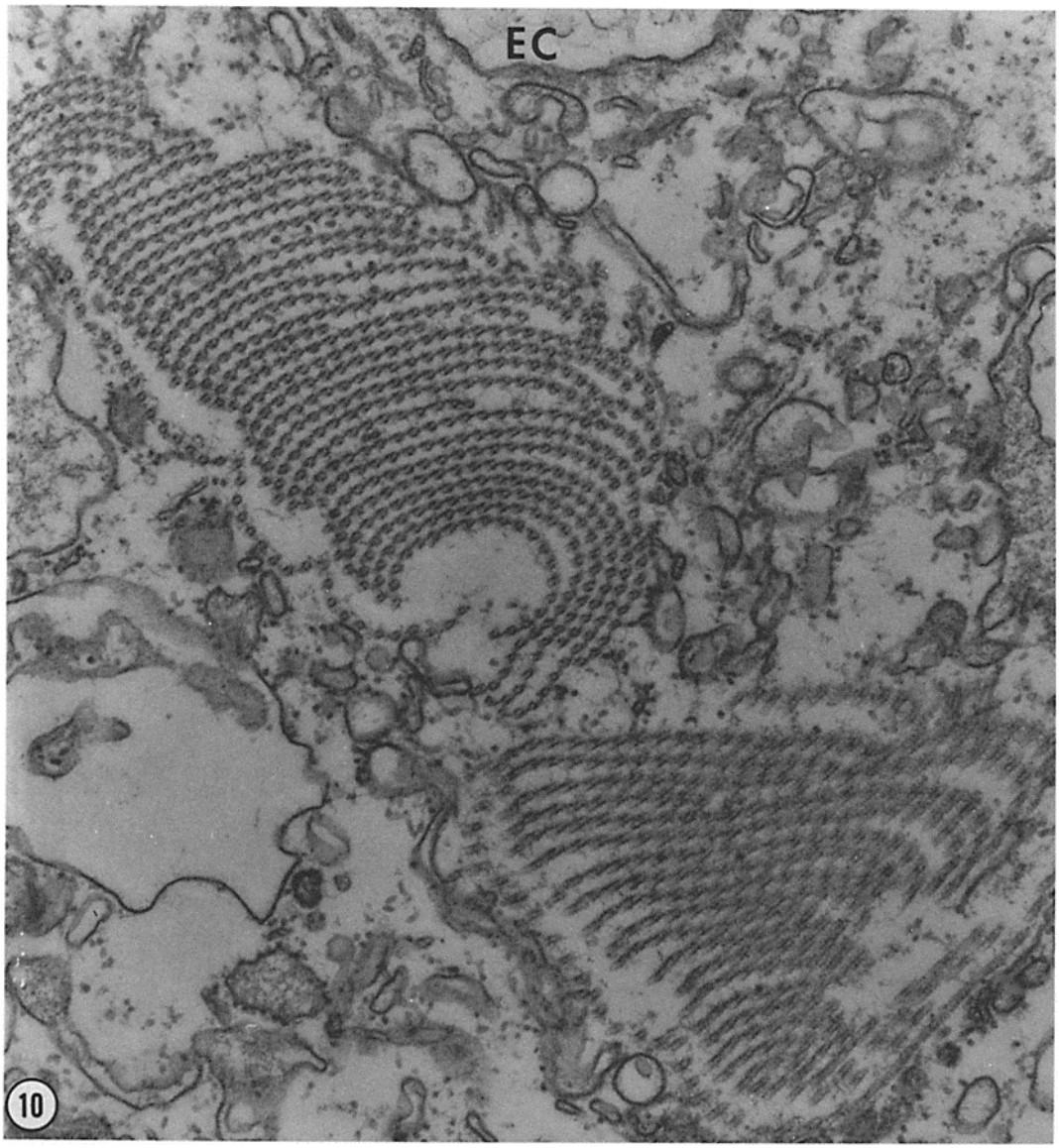

FIGURE 10 Electron micrograph cross-section of an axostyle that is split into two pieces. The splitting occurs between rows and usually not within rows. *EC*, extracellular space. × 54,000.

and this "modified" wave usually does not propagate. As a result, sinelike waves accumulate in the irradiated area (Fig. 11). At times, when enough waves arrive at that area to fill it, some "slip through" in spurts and continue into the distal end of the axostyle (Fig. 11). It appears as though waves entering the affected region push along, or stimulate the propagation of waves accumulated there. The distal end then beats as a sawtooth wave, indicating that only the irradiated region of the axostyle is altered. The usual cessation of propagation of the short wavelength sinelike waves in the irradiated area makes it appear as though the irradiated area has acquired a higher viscosity or stiffness, and the waves have greater difficulty traversing that region. A slight degree of reversibility is sometimes observed in the irradiated area, but generally the effect is not reversible.

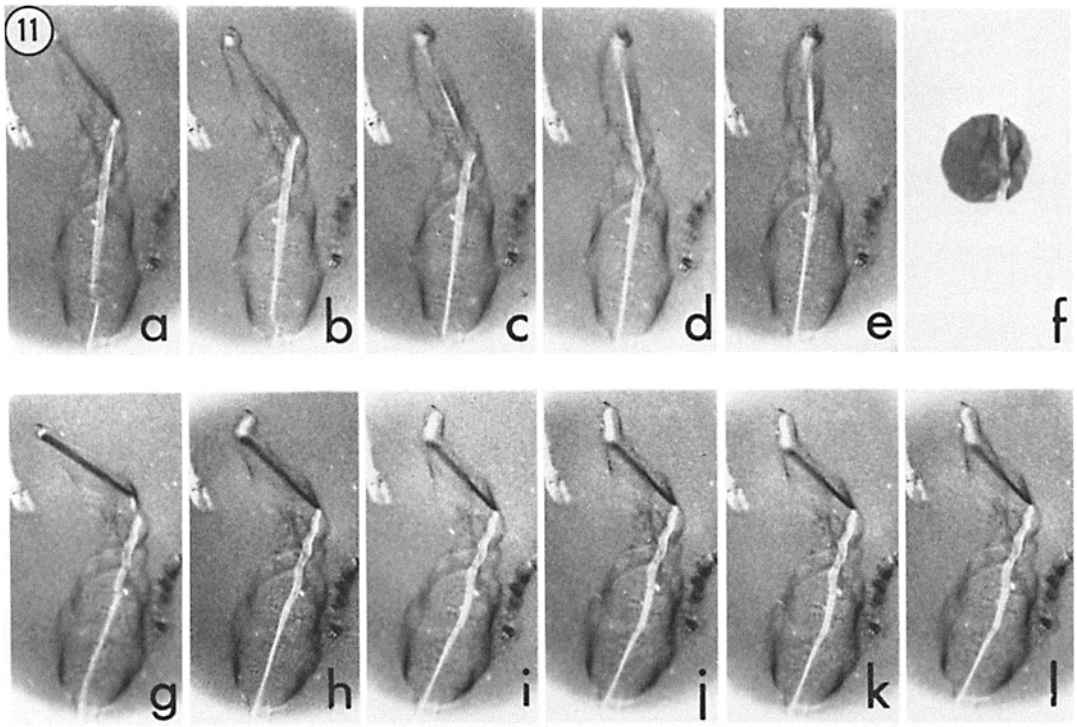

FIGURE 11 Polarized light micrographs of an axostyle irradiated with a microbeam of blue light. The first row of micrographs (*a–e*) shows the normal beating axostyle. Micrograph *f* shows the area of the axostyle irradiated with the blue light microbeam. The second row of micrographs (*g–l*) shows the effect of the irradiation. In the area irradiated, short sine waves accumulate and fill the region. Waves that slip through the microbeamed region assume the normal sawtooth waveshape. There is no reduction of birefringence in the area irradiated. Sequential frames, 18 frames/s. × 500.

Once the propagation stops in the affected region, very seldom does it start up again. When waves can no longer slip through the irradiated region, a wave sometimes spontaneously starts from the distal end of the axostyle and travels up to that region. A rough estimation of the action spectrum for this effect was determined by using either a blue, green, or red glass filter over the light source when irradiating cells. Wave modification was observed only when the axostyle was irradiated with blue light. We therefore describe this modification as a blue light effect.

IRRADIATION WITH ULTRAVIOLET: An axostyle irradiated with a microbeam of UV light responds differently than when irradiated with blue light. UV light severs the axostyle into two pieces (Fig. 12). The birefringence in the microbeamed region disappears, which means that the elements responsible for the birefringence, i.e., the microtubules, must have broken down. The anterior end continues to initiate and propagate waves, the posterior half does not. Short exposures to UV, insufficient to sever the axostyle, sometimes caused waves to stop short of the irradiated region. Low dosages of UV did not, however, duplicate the blue light effect.

A surprising observation was made after some of the axostyles were severed with UV. In several cases, the severed ends began to move together. This movement did not appear to be passive, resulting from forces in the cell cytoplasm or cell surface, but to be movement resulting from activity in the irradiated region itself. This apparently "active" movement could be explained if there were a few microtubules connecting the two severed pieces that could serve as elements for somehow moving the pieces together.

An interesting phenomenon occurs when an axostyle is severed in two places, separated by about one wavelength. The short segment pro-

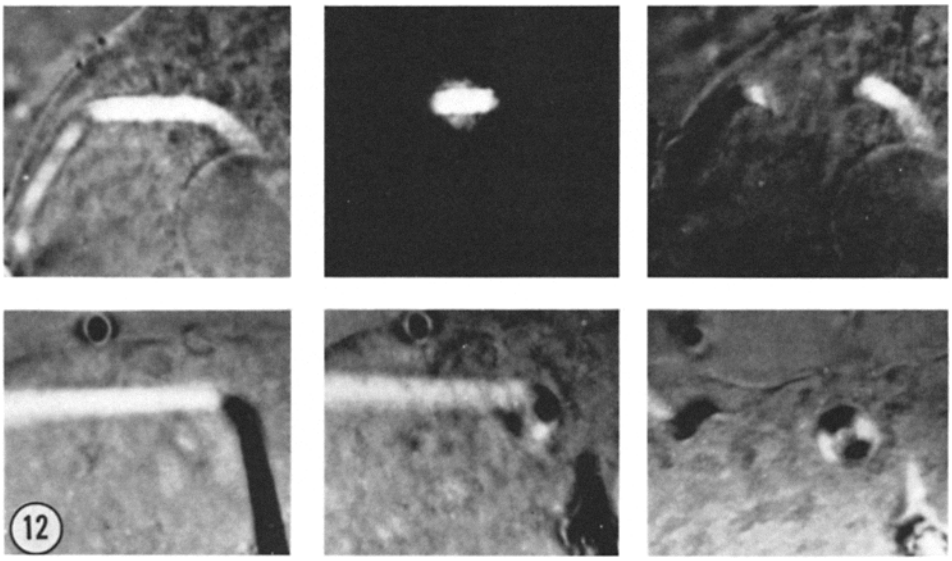

FIGURE 12 Polarized light micrographs of the axostyle irradiated with a UV microbeam. The top row of three micrographs indicates before, during, and after irradiation. Before irradiation, the axostyle had stopped beating. After irradiation, the birefringence in the microbeamed region is gone, and the severed ends curl. The bottom row of three micrographs shows an axostyle that has been irradiated at two points on either side of a bend that had momentarily stopped on the axostyle. The third micrograph of this series shows that the short piece curls upon itself to form a lock-washer with radius similar to normal bend radius. (The ends are displaced in the plane perpendicular to the plane of the photograph.) × 1,200.

duced by the UV microbeam curls upon itself into a lock-washer configuration (Fig. 12). This curling phenomenon was also observed at the two ends, produced when the axostyle is severed in only one place. The ability to curl is significant in that the mechanism may be similar to that involved in wave formation.

DISCUSSION

Cilia- and Flagella-like Movements of the Axostyle

The ribbon-shaped axostyle of *Pyrsonympha* contains a highly ordered bundle of microtubules. The semicrystalline organization of the microtubules of this axostyle has permitted an analysis of its movements in vivo. In cross-section, the axostyle is ~3 × wider than thick and hence the retardation, as measured with the polarized light microscope, varies according to whether the light beam passes through the width or thickness of the axostyle. Therefore it has been possible to deduce the exact three-dimensional waveform of the axostylar motion by coupling polarized light microscopy and cinematography.

We show that the axostyle has both cilia- and flagella-like movements. As with a beating cilium (29), the bending of the anterior one-fifth of the axostyle has a recovery and an effective phase. Much like the principal and reverse bends of flagella (16), the propagating waves contain two contiguous arcs with curvature in opposite directions. These S-shaped bends or arcs are separated by straight regions, the net appearance being that of sawtooth-shaped waves that flow rhythmically along the axostyle.

The bends on the *Pyrsonympha* axostyle were previously described by Smith and Arnott (31) as half sine waves. This term does not adequately describe the entire wave form which contains both a bent and a straight region. Therefore, the more descriptive term, sawtooth waves, was adopted in this paper.

The flexual bending of the anterior part of the axostyle develops the sawtooth wave and causes the anterior tip of the organism to precess. The propagating sawtooth waves cause the axostyle to roll back and forth about its long axis. The precessional and rotational movements occur because the axostyle is intrinsically twisted into a

helix of low pitch.

The propagating bends are nearly planar and the twist in the axostyle appears to dissipate in the region of the bend. Three or four sawtooth waves travel along the axostyle at any given time at an average velocity of 40 μm/s. The velocity varies along the axostyle apparently because of differences in the physical conditions that the waves experience.

The undulations in the axostyle in *Pyrsonympha* and *Saccinobaculus* resemble each other but differ in several respects. In both organisms, the axostyle bends to produce a circular arc which propagates down the twisted organelle. Each wave in the axostyle of *Pyrsonympha*, however, contains two arcs with opposite curvature while the wave in the axostyle in *Saccinobaculus* usually contains a single propagating arc (25). The radii of the arcs on the two axostyles differ too. In *Saccinobaculus*, the axostyle bends to a radius of ~8 μm with an arc ranging from 60° to 180°, while in *Pyrsonympha* the axostyle forms two, sharp, contiguous arcs, each with a radius of ~1.4 μm and each with an arc ranging from 40° to 60°. In *Saccinobaculus*, therefore, a larger portion of the axostyle is included in each bend than is true in *Pyrsonympha*.

The Plane of Bending in the Axostyle and the Position of the Dynein Cross-Bridges

The plane of bending in relation to the alignment of the microtubular rows differs in the axostyles of *Saccinobaculus* and *Pyrsonympha*. In *Pyrsonympha*, we show that the plane of the bend is perpendicular to the width of the axostyle. The diagram in Fig. 5 shows orthogonal axes labeled x, y, and z representing the width, height, and length of the axostyle, respectively. In cross-section, microtubular rows appear in succession along the x axis (Fig. 5). The microtubular rows themselves lie in the y–z plane. The bending also takes place in the y–z plane. This means that bending is parallel to the plane of the rows and that microtubules within a row must be displaced relative to one another during bending. This situation does not pertain in the axostyle in *Saccinobaculus*. There, the plane in which bending occurs is perpendicular to the axostyle's width and to the plane that contains the rows of microtubules. Therefore, in the *Saccinobaculus* axostyle, relative sliding of rows is expected.

Since bending is parallel to the rows in the axostyle of *Pyrsonympha*, adjacent microtubules within a row must be displaced during bending. This means that the intrarow cross-bridges must either detach or deform during the bending process. On the basis of electron microscope observations, Smith and Arnott (31) report that in the bend region of the *Pyrsonympha* axostyle the intrarow cross-bridges appear not to completely span the space between adjacent microtubules within a row. This observation may suggest that intrarow cross-bridges detach during bending.

On the other hand, the intrarow cross-bridges may not detach but stretch to accommodate the bend. This would require that the intrarow cross-bridges stretch to about twice their rest length or by ~20 nm. This is the maximum displacement that should develop between adjacent microtubules within a row when the axostyle bends to a radius of curvature in the y–z plane of 1.5 μm and forms an arc which extends over 60°. In fact, such an elastic deformation may even explain the S-shape of the bend. The possibility exists that the B curvature forms to relieve the strain on the intrarow bridges produced by the A curvature. Elastic deformation of the intrarow cross-bridges may be coupled with contraction of the tubules on the inside of the bend. Microtubule contraction has been demonstrated in the axostyle of *Saccinobaculus* (25).

The position of the dyneinlike bridges in the *Pyrsonympha* axostyle has not been firmly established. The difficulty in establishing this fact is a result of the inability to grow these anaerobic protozoa in culture so as to obtain enough cells for biochemical studies. The existing evidence suggests, however, that the dyneinlike enzyme is in the intrarow bridges (2, 26) and that nexin is in the intrarow bridges (26). These data are tenuous at best and are based principally on the appearance of the cross linkers in electron micrographs. Dyneinlike bridges are thought to be more delicate and less regular in appearance than structural bridges.

If the dyneinlike cross bridges generate force within the bend regions of the axostyle, these force-producing cross-bridges should be perpendicular to the width. The one set of bridges, which are aligned at 90° to the width of the axostyle and are delicate in appearance like putative dynein bridges, are the linkers which connect a single row of tubules running along the inner face of the axostyle to the rest of the axostyle. This row of tubules, seen in the cross-sections of the axostyle

in Figs. 4 and 10, has strong (intrarow) bridges parallel to the width and weaker, more irregular bridges normal to the width of the axostyle. These delicate bridges attached to this row have the proper orientation to serve as the force-generating cross-bridges for bending. However, force generation may not occur in the bend region as will be discussed below.

The uniform distribution of dyneinlike cross-bridges along the axostyle is supported by observation of the wave motion in the *Pyrsonympha* axostyle. We show that sawtooth waves initiate from any point on the axostyle including the distal end, an observation that corroborates the observation of others (4, 31). In addition, we show that the amplitude of the bend curvature is not dampened as waves propagate, and that waves can speed up in transit after having been slowed by blue light irradiation or by physical constraints in the cytoplasm of the cell or in the medium. These observations suggest that the dyneinlike force-producing cross-bridges (14, 17) which convert chemical energy into mechanical work are uniformly distributed along the axostyle.

We show that the sawtooth waves contain two contiguous arcs with curvature in opposite directions. This could mean that each active cross-bridge can generate force in either direction depending on the direction of curvature. This possibility has generally not been favored (5, 6) because it is inconsistent with our knowledge of the properties of the cross-bridges in striated muscle, in which case the myosin heads are polarized and are believed to only generate force in one direction. However, our data from the axostyle of *Pyrsonympha* strongly suggest that active sliding in either direction is possible.

The propagation of sawtooth waves becomes more difficult to explain on the basis of unidirectional force generation when one considers that waves sometimes reverse propagation direction without wave shape reversal. We observed that, when the direction of movement of some waves reversed, the relationships of the arcs remained unchanged so that the leading arc (arc B) before the reversal maintained its negative curvature as it became the trailing arc after reversal. This reversal of propagation without a concomitant wave shape reversal again suggests that active sliding in either direction is possible.

The microtubules of the axostyle in *Pyrsonympha* originate from an anteriorly placed axial ribbon (4, 7, 20, 31). Unlike axonemal microtubules whose proximal ends are anchored by a basal body, the proximal ends of the axostylar microtubules are simply embedded in an amorphous matrix. The nature of the amorphous material around the tubule ends is unclear, but the lack of a basal-body-like attachment may permit displacement of the tubule ends at the proximal tip. The absence of a basal-body attachment of the axostylar microtubules at the proximal end, in contrast to the situation which pertains in cilia and flagella, may be an important consideration for axostyle movement.

Perturbations of Axostyle Motility

The motions of the axostyle are perturbed by UV and blue light microbeam irradiation and other environmental factors such as changes in temperature. These perturbations are of interest because they help identify constraints on models that are devised to explain the mechanism and coordination of bending. One important modifier of axostyle motility is temperature, and we report here that velocity and wave initiation respond differently to changes in temperature. When the temperature of the medium is lowered to 5°C for a short time and then returned to 21°C, wave velocity returns to normal before frequency does. This is interpreted to mean that the factor(s) which controls the initiation event (an ionic gradient perhaps) is different from the factor which controls the on-off activity of the cross-bridges (bend curvature perhaps). If cross-bridge control is mechanical (6) while wave initiation is chemical, one may expect that the cell membrane or vesicle membranes which regulate the ionic gradient are sensitive to temperature while the mechanical events would not be.

Blue light, another perturbant of axostyle motility, affects both velocity and wave form simultaneously. The waves which accumulate in the irradiated region arise as and are similar in form to the A and B arcs which travel into that region. The birefringence of the irradiated region does not change, suggesting that the microtubules themselves are intact. Our data do not allow us to determine which of the two sets of bridges, if either, is affected. Nevertheless, the fact that wave form and velocity revert to normal beyond a blue light-affected region of the axostyle strongly suggests that the factors which regulate wave form and velocity are local properties of the axostyle.

The blue light effect is likely a result of the

presence of a photosensitizer of either an endogenous or exogenous source in close association with the axostyle. The photosensitizer appears to be intimately associated with the axostyle because the response to irradiation is rapid and irradiation of the cytoplasm near, but not including, the axostyle does not produce a response. Birefringence of the axostyle is not affected by blue light and, therefore, the overall structure of the microtubules is not affected. The blue light response is definitely not a result of a local increase in temperature. Using, as a model, a liquid crystal whose color changes sensitively with temperature (27), we found no temperature increase by the same dosages of irradiation. In addition, when a theoretical calculation is made based on the spot size of the microbeam and the conductive properties of water, we determined that the energy available is insufficient to raise the temperature anywhere near 1°C.

A microbeam of UV light severs the axostyle in two, and the severed ends can coil into circular arcs much like the arcs which propagate on the axostyle. The coiling of microtubules at the severed ends may be the result of the tendency of tubules to coil when not otherwise restrained (12) or the result of active cross-bridges which normally produce sliding.

Perturbations, which are not yet clear to us, cause the axostyle to lose stiffness. The reduction in stiffness results in a larger radius of bending which occurs in a region of the axostyle near the nucleus. This region of the axostyle is where the second of the two arcs of a sawtooth wave (arc B) forms and the flexual motion becomes undulatory. The loss of stiffness may reflect a loss of curvature of the microtubular rows and a loss of the crescent or cupped shape of the axostyle.

The Position of Force Production in the Sawtooth Waves

The position of active force production in the axostyle of *P. vertens* is of special interest. If one accepts the assumption that force is produced by the interrow cross-bridges and that relative sliding of microtubular rows takes place, it is possible that active sliding between microtubular rows may not take place in the S-shaped bends but rather in the non-bent segments of the axostyle. While intuitively the S-shaped bends may appear to be the active regions (in analogy with the bends of sperm flagella, for example), the following observations on the axostyle and a ribbon model of the axostyle suggest that the converse may, in fact, be true.

The rows of microtubules in the axostyle of *P. vertens* are straight (orthogonally arranged) in cross-sections of bends, and the axostyle bends in a plane which includes the straight rows, rather than at right angles to the rows. Conversely, in the unbent segments of the axostyle, the microtubular rows are curved and the cross-section of the axostyle itself is cupped. Therefore, corresponding microtubules in adjacent rows are displaced relative to their arrangement in the bend region. Given these observations, a model which simulates the beating axostyle can be made from a flexible ribbon of paper. A 2-cm wide ribbon of bond paper, ~30 cm long, is considerably stiffer when its cross-section is cupped (and its moment increased) compared to when it is not cupped, but flat. (Consider the rigidity of a thin metal tape measure [25] which becomes flat and more easily bent when an external bending force exceeding a critical value is applied.) The flat ribbon of paper held upright at its base cannot support its own weight and will bow at its base. If at the ribbon's base a curvature along the width of the ribbon is introduced by squeezing the width of the ribbon, the moment of the ribbon increases and the ribbon erects itself progressively from the base upwards. The bend travels upwards as the ribbon is squeezed. When the moment is reduced by squeezing the ribbon less, the ribbon can no longer support itself and the bend travels down. Such a progressive stiffening, which results in the travel of a bend, seems precisely to take place rhythmically at the rostral end of the axostyle where arc A is formed.

Now, if the paper ribbon model is constrained by loosely holding the distal end of the ribbon in a horizontal direction, then a second bend equivalent to arc B appears as arc A is made to travel from the base upwards. If the ribbon is somewhat twisted, a back and forth rotation of it coupled with rhythmically increased stiffness induced at its base, sends a flipping sawtooth wave down the length of the ribbon. This model flips in a lifelike imitation of the beating axostyle in *P. vertens*.

We may thus conjecture that the sawtooth wave in the axostyle of *P. vertens* is generated by interrow cross-bridges which are active in the straight regions. The active cross-bridges curve the microtubular rows and cup the axostyle, thereby stiffening the latter. The axostyle, upon

encountering its own twist and the imposed internal and cytoplasmic constraints, assumes the A and B arcs of the S-shaped bend which is pushed ahead of the active stiff (straight) region. We might then interpret the several bends, accumulated in the blue light-irradiated region, as bends which pile up in the absence of active sliding between interrow tubules or as the inability of interrow linkers to dissociate or reassociate.

In conclusion, the axostyle is shown to have many features in common with cilia and flagella but to be simpler in structure and organization and therefore to be a good model of microtubule-associated movement. Since the axostyle in *Pyrsonympha* exhibits both cilia- and flagella-like behavior, this dualism further emphasizes the similarities between these two bending processes. The axostyle has a semicrystalline arrangement of microtubules, and therefore it may be suitable for analysis by x-ray diffraction. Studies which will expand our knowledge of the composition of each of the different cross-bridges within the axostyle will significantly help understand the mechanism which localizes and coordinates bending in the axostyle. A radial spoke-central sheath complex is not required for bend formation, since these structures are not present in the axostyle.

We thank Dr. T. Punnett for his help with the formulation of the protozoan medium, Mrs. Bush for her expert technical assistance with electron microscopy, Ira Sabran for his contributions to the UV microbeam experiments, and Drs. G. Ellis and H. Sato for their continued advice and assistance during the course of this work.

This work was partly supported by National Institutes of Health (NIH) Postdoctoral Fellowship GM 49352 and Marine Biological Laboratory, (MBL) Steps Toward Independence Fellowship to G. Langford; NIH grant CA 10171 and National Science Foundation grant GB 31739 awarded to S. Inoué.

Received for publication 15 September 1978, and in revised form 30 October 1978.

REFERENCES

1. Ballantine, R. 1954. High efficiency still for pure water. *Anal. Chem.* **26**:549–550.
2. Bloodgood, R. A. 1975. Biochemical analysis of axostyle motility. *Cytobios.* **14**:101–120.
3. Bloodgood, R. A., and K. R. Miller. 1974. Freeze-fracture of microtubules and bridges in motile axostyles. *J. Cell Biol.* **62**:660–671.
4. Bloodgood, R. A., K. R. Miller, T. B. Fitzharris, and J. R. McIntosh. 1974. The Ultrastructure of *Pyrsonympha* and its associated microorganisms. *J. Morphol.* **143**:77–106.
5. Brokaw, C. J. 1971. Bend propagation by a sliding filament model for flagella. *J. Exp. Biol.* **55**:289–304.
6. Brokaw, C. J. 1972. Flagellar movement: a sliding filament model. *Science (Wash. D. C.).* **178**:455–462.
7. Brugerolle, G. 1970. Sur l'ultrastructure et la position systematique de *Pyrsonympha vertens* (Zooflagellata Pyrsonymphina). *C. R. Hebd. Seances Acad. Sci. Ser. D. Sci. Nat.* **270**:966–969.
8. Cleveland, L. R. 1923. Correlation between the food and morphology of termites and the presence of intestinal protozoa. *Am. J. Hyg.* **3**: 444.
9. Cleveland, L. R. 1924. The physiological and symbiotic relationships between the intestinal protozoa of termites and their host, with special reference to *Reticulitermes flavipes* Kollar. *Biol. Bull. (Woods Hole).* **46**:178–201.
10. Cleveland, L. R. 1950. Hormone-induced sexual cycles of flagellates. III. Gametogenesis, fertilization, and one-division meiosis in *Saccinobaculus*. *J. Morphol.* **86**:215–227.
11. Cleveland, L. R., S. R. Hall, E. P. Saunders, and J. Collier. 1934. The wood-feeding roach, *Cryptocercus*, its protozoa, and the symbiosis between protozoa and roach. *Mem. Am. Acad. Arts Sci.* **17**: 185–342.
12. Costello, D. P. 1973. A new theory on the mechanics of ciliary and flagellar motility. II. Theoretical considerations. *Biol. Bull. (Woods Hole).* **145**:292–309.
13. Fitzharris, T. R., R. A. Bloodgood, and J. R. McIntosh. 1972. The effect of fixation on the wave propagation of the protozoan axostyle. *Tissue Cell.* **4**:219–225.
14. Gibbons, I. R. 1963. Studies on the protein components of cilia from *Tetrahymena pyriformis*. *Proc. Natl. Acad. Sci. U. S. A.* **50**:1002–1010.
15. Gibbons, I. R. 1977. Structure and function of microtubules. *In* International Cell Biology 1976–1977. B. R. Brinkley and K. R. Porter, editors. The Rockefeller University Press, New York. 348–357.
16. Gibbons, B. H., and I. R. Gibbons. 1972. Flagellar movement and adenosine triphosphatase activity in sea urchin sperm extracted with Triton X-100. *J. Cell Biol.* **54**:75–97.
17. Gibbons, I. R., and A. J. Rowe. 1965. Dynein: a protein with adenosine triphosphatase activity from cilia. *Science (Wash. D. C.).* **149**:424–426.
18. Grasse, P. P. 1956. L'ultrastructure de *Pyrsonympha vertens* (zooflagellata Pyrsonymphina): les flagelles et leur coaptation avec le corps, l'axostyle contractile, le paraxostyle, le cytoplasme. *Arch. Biol.* **67**: 595–611.
19. Grimstone, A. V., and L. R. Cleveland. 1965. The fine structure and function of the contractile axostyles of certain flagellates. *J. Cell Biol.* **24**:387–400.
20. Hollande, A., and J. Carruette-Valentin. 1970. La lignee des Pyrsonymphines et les caracteres infrastructuraux communs aux genres *Opisthomitus*, *Oxymonas*, *Saccinobaculus*, *Pyrsonympha* et *Steblomastix*. *C. R. Hebd. Seances Acad. Sci. Ser. D Sci. Nat.* **270**:1587–1590.
21. Kamiya, N. 1959. Protoplasmic streaming. *Protoplasmatologia.* **3a**: 150–155.
22. Langford, G. M. 1975. The plane of bending in the axostyle of *Pyrsonympha vertens*. *Biosystems.* **7**:370–371.
23. Langford, G. M., S. Inoue, and I. R. Sabran. 1973. Analysis of axostyle motility in *Pyrsonympha vertens*. *J. Cell Biol.* **59**(2, Pt. 2): 185 a. (Abstr.).
24. McIntosh, J. R., E. S. Ogata, and S. C. Landis. 1973. The axostyle of *Saccinobaculus*. I. Structure of the organism and its microtubule bundle. *J. Cell Biol.* **56**:304–323.
25. McIntosh, J. R. 1973. The axostyle of *Saccinobaculus*. II. Motion of the microtubule bundle and a structural comparison of straight and bent axostyles. *J. Cell Biol.* **56**:324–339.
26. Mooseker, M. S., and L. G. Tilney. 1973. Isolation and reactivation of the axostyle: Evidence for a dynein-like ATPase in the axostyle. *J. Cell Biol.* **56**:13–26.
27. Nicklas, R. B. 1973. Methods for gentle, differential heating of part of a single living cell. *J. Cell Biol.* **59**:595–600.
28. Provasoli, L. 1958. Nutrition and ecology of protozoa and algae. *Ann. Rev. Microbiol.* **12**:279–308.
29. Sleigh, M. 1968. Patterns of ciliary beating. *Symp. Soc. Exp. Biol.* **22**:131–150.
30. Smith, H. E. 1970. Axostyle structure and function in *Pyrsonympha vertens* with description of flagella, scales, and associated microorganisms. Ph.D. Thesis. University of Texas at Austin, Austin, Texas.
31. Smith, H. E., and H. J. Arnott. 1974. Axostyle structure in the termite protozoa *Pyrsonympha vertens*. *Tissue Cell.* **6**:193–207.
32. Stephens, R. E., and K. T. Edds. 1976. Microtubules: structure, chemistry and function. *Physiol. Rev.* **56**:709–777.
33. Summers, K. E., and I. R. Gibbons. 1971. Adenosine triphosphate-induced sliding of tubules in trypsin-treated flagella of sea-urchin sperm. *Proc. Natl. Acad. Sci. U. S. A.* **68**:3092–3096.
34. Warner, F. D., and P. Satir. 1974. The structural basis of ciliary bend formation: radial spoke positional changes accompanying microtubule sliding. *J. Cell Biol.* **63**:35–63.